Mon. Not. R. Astron. Soc. **393,** 108–112 (2009) doi:10.1111/j.1365-2966.2008.14135.x

Sakurai's Object: characterizing the near-infrared CO ejecta between 2003 and 2007

H. L. Worters,[1,2⋆] M. T. Rushton,[1] S. P. S. Eyres,[1] T. R. Geballe[3] and A. Evans[4]

[1] *Centre for Astrophysics, University of Central Lancashire, Preston PR1 2HE*
[2] *South African Astronomical Observatory, Observatory, 7935, South Africa*
[3] *Gemini Observatory, 670 N. A'ohoku Place, Hilo, HI 96720, USA*
[4] *Astrophysics Group, Keele University, Keele, Staffordshire ST5 5BG*

Accepted 2008 October 23. Received 2008 October 22; in original form 2008 May 21

ABSTRACT

We present observations of Sakurai's Object obtained at 1–5 μm between 2003 and 2007. By fitting a radiative transfer model to an echelle spectrum of CO fundamental absorption features around 4.7 μm, we determine the excitation conditions in the line-forming region. We find $^{12}C/^{13}C = 3.5^{+2.0}_{-1.5}$, consistent with CO originating in ejecta processed by the very late thermal pulse, rather than in the pre-existing planetary nebula. We demonstrate the existence of $2.2 \times 10^{-6} \leq M_{CO} \leq 2.7 \times 10^{-6}\,M_{\odot}$ of CO ejecta outside the dust, forming a high-velocity wind of 500 ± 80 km s^{-1}. We find evidence for significant weakening of the CO band and cooling of the dust around the central star between 2003 and 2005. The gas and dust temperatures are implausibly high for stellar radiation to be the sole contributor.

Key words: stars: abundances – stars: AGB and post-AGB – circumstellar matter – stars: individual: V4334 Sgr – stars: individual: Sakurai's Object – stars: winds, outflows.

1 INTRODUCTION

Sakurai's Object is a highly evolved post-asymptotic giant branch (post-AGB) star that had begun to venture down the white dwarf cooling track when, in 1995, it underwent sudden rebrightening (Nakano et al. 1996) due to a final helium shell flash, or very late thermal pulse (VLTP) (Duerbeck et al. 1997). Since then, Sakurai's Object has undergone observable changes on time-scales of weeks to months, providing an instance in which this very brief stage of evolution experienced by ∼15 per cent of intermediate-mass stars (Iben, Tutukov & Yungelson 1996) could be tracked over a period of only a few years. Several phases of dust production followed the outburst, with a deep optical minimum beginning in early 1999, such that any changes in the central star have since been inferred from radio and infrared observations (Tyne et al. 2000; Hajduk et al. 2005; van Hoof et al. 2007). Subsequent observations and modelling have revealed much about the dust shell formation and the outer regions of the ejecta (e.g. Kimeswenger & Koller 2002; Tyne et al. 2002).

Using observations at 2.3 μm from 1998, Pavlenko et al. (2004) modelled overtone CO band absorption in the stellar atmosphere to determine a $^{12}C/^{13}C$ ratio of 4 ± 1, consistent with VLTP nucleosynthesis. In order to follow the development of the ejecta, annual monitoring of the target in the near-infrared has been undertaken. The discovery of fundamental band (4.7 μm) lines of CO in the wind was reported by Eyres et al. (2004), based on a low-resolution spectroscopy obtained in 2002 and 2003. Here, we present the analysis of observations of the CO fundamental lines in data obtained between 2003 and 2007, mostly at higher resolution.

2 OBSERVATIONS

All data presented here were obtained at the United Kingdom Infrared Telescope (UKIRT) on Mauna Kea, Hawaii, using the facility spectrographs CGS4 and UIST. A summary of the observations is given in Table 1. Low-resolution spectra were predominantly obtained with UIST, utilizing the 0.24 and 0.48 arcsec slits, but in one instance (2005 August 3) CGS4 and its 0.61 arcsec slit were used. For all the observations, the telescope was nodded in the standard ABBA pattern. Standard stars were observed just prior to or after Sakurai's Object and at airmasses close to those of the target. The spectra of Sakurai's Object were ratioed by those of the appropriate calibration stars (Table 1). Flux calibration was performed utilizing photometry of the standard stars and colour corrections based on Tokunaga (2000). Wavelength calibration was obtained from an arc lamp or telluric absorption lines in the spectrum of the calibration star, and was accurate to better than 0.0001 μm for the UIST and low-resolution CGS4 spectra.

In the case of the CGS4 echelle observations on 2004 June 10, three echelle settings were used with a slit width of 0.9 arcsec to

⋆E-mail: hannah@saao.ac.za

Table 1. Log of near-infrared spectroscopic observations obtained with UKIRT and presented in this paper. An asterisk denotes an observation made with CGS4; all remaining spectra were acquired using UIST.

Date	t_{int} (s)	Waveband (μm)	R	Calibration star Name	Spectral type
2003 September 8	720	1.40–2.51	500	HIP 86814	F6V
2003 September 8	480	2.91–3.64	1400	BS 6378	A2IV–V
2003 September 8	240	3.62–4.23	1400	BS 6378	A2IV–V
2003 September 8	960	4.38–5.31	1200	BS 6378	A2IV–V
2004 June 10	1200	1.40–2.51	2000	HIP 86814	F6V
2004 June 10	840	2.23–2.99	2000	HIP 86814	F6V
2004 June 10	1440	2.91–3.64	2000	BS 6378	A2IV–V
2004 June 10	720	3.62–4.23	2000	BS 6378	A2IV–V
2004 June 10	1120	4.38–5.31	2000	BS 6496	F5V
2004 June 10*	600	4.678–4.692	20000	BS 6378	A2IV–V
2004 June 10*	600	4.713–4.727	20000	BS 6378	A2IV–V
2004 June 10*	510	4.758–4.762	20000	BS 6378	A2IV–V
2005 August 3*	560	4.48–5.12	2000	BS 6595	F5V
2007 June 2	1080	3.62–4.23	2000	BS 6595	F5V
2007 June 2	2400	4.38–5.31	2000	BS 6595	F5V

cover the wavelength range 4.68–4.77 μm at a resolving power of 20 000 (15 km s^{-1}). Following data reduction, the three spectra were adjoined after applying small scaling factors to two of the spectra in order to match the continuum levels. Wavelength calibration for these spectra was derived from telluric CO lines and is accurate to 3 km s^{-1}.

3 RESULTS

Fig. 1(a) shows spectra of Sakurai's Object in the 1–5 μm region from 2003 to 2007. The continuum can be seen to fade from one year to the next, with a substantial decrease in flux density between the 2004 and 2005 observations. To aid comparison of the continuum shapes, Fig. 1(b) shows the 2005 and 2007 spectra scaled up by a factor of 14. Vertical offsets have also been applied to the 2004, 2005 and 2007 spectra for display purposes. A difference in gradient of the continua can be seen, particularly in the *M* band, indicating a blackbody peak at increasing wavelength in consecutive years, strongly suggesting cooling of the dust. The only features superimposed upon the continuum are the fundamental absorption lines of CO around 4.7 μm. These can be seen in Fig. 1(c); an enlargement of the ^{12}CO P-branch and ^{13}CO R-branch region. The 2004, 2005 and 2007 low-resolution spectra have been convolved with a Gaussian profile of a full width at half-maximum (FWHM) equal to the resolution of the 2003 spectrum. Comparing the spectra, one can see a significant weakening of the CO band from 2003 to 2005. Although individual lines cannot clearly be seen in the 2005 spectrum, the apparent emission bump at 4.67 μm, the wavelength of the CO band centre, is a strong indication that weak P- and R-branch absorption lines are still present. The low signal-to-noise ratio of the 2007 spectrum precludes a meaningful estimate of the CO band strength.

Fig. 2 is the echelle spectrum from 2004 June, showing ^{12}CO and ^{13}CO in absorption around 4.7 μm. The absorption features have non-Gaussian profiles and show remarkably large linewidths. We measure a full width at zero intensity (FWZI) of 400 ± 70 km s^{-1} and FWHM of 180 ± 15 km s^{-1}. By measuring the blueshift of absorption features in the echelle spectrum, we can improve upon the 290 ± 30 km s^{-1} absorption maximum found by Eyres et al. (2004) using observations made at lower resolution. After correcting for the heliocentric radial velocity of +115 km s^{-1} (Duerbeck & Benetti 1996), we find the velocity of the absorption maximum to be 270 ± 15 km s^{-1} relative to the star.

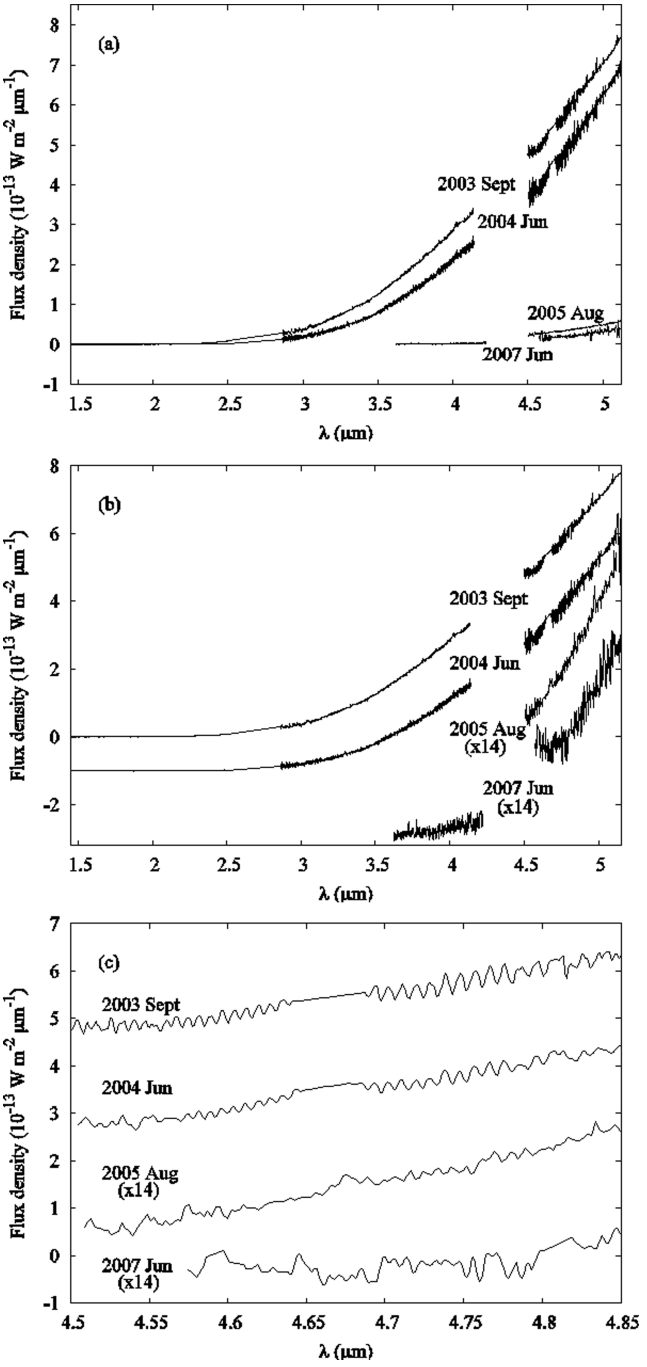

Figure 1. (a) UKIRT spectra of Sakurai's Object on 2003 September 8, 2004 June 10, 2005 August 3 and 2007 June 2. Gaps occur in the data due to strong telluric absorption. (b) The same UKIRT spectra shown in (a), with 2005 and 2007 spectra scaled up by a factor of 14 to aid comparison of continuum shapes. Spectra from 2004, 2005 and 2007 have been offset vertically by −1, −3 and −3 × 10^{-13} W m^{-2} μm^{-1}, respectively. (c) An enlargement of (b) over the spectral range of the ^{12}CO P-branch and ^{13}CO R-branch lines. The 2003 and 2004 spectra are interpolated between 4.64 and 4.68 μm because of two strong hydrogen absorption lines in the spectrum of the A2 calibration star.

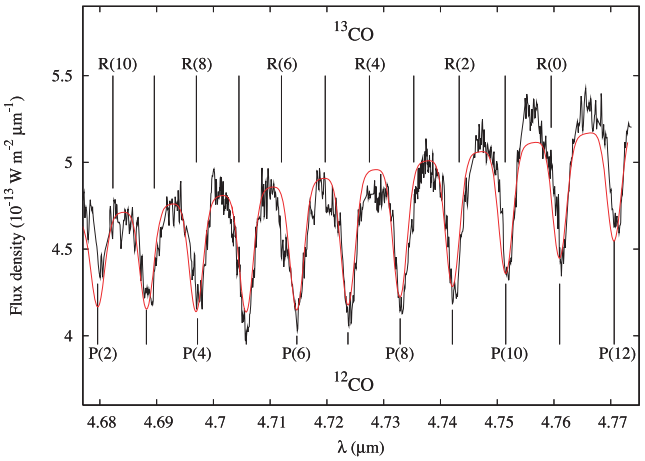

Figure 2. UKIRT echelle spectrum of CO (1–0) absorption in Sakurai's Object from 2004 June 10. ^{12}CO P-branch and ^{13}CO R-branch lines are labelled; the wavelengths of the lines are for a stellar radial velocity of +115 km s^{-1} and peak absorption at a heliocentric velocity of −270 km s^{-1}. The smooth red line superimposed upon the spectrum corresponds to a spherical shell model spectrum consisting solely of ^{12}C^{16}O.

4 MODELLING THE CO

In order to ascertain whether the CO detected outside the dust in 2004 originates in ejecta from the central star observed by Pavlenko et al. (2004), or is associated with the old planetary nebula (PN) or interstellar medium (ISM), we estimate the ^{12}C/^{13}C isotopic ratio by applying a simple radiative transfer model to the 4.68–4.78 μm echelle spectrum, shown in Fig. 2. Because the absorption features are extremely broad, the ^{13}CO lines are blended with the stronger ^{12}CO lines. Their presence has a tangible effect on the spectrum. There is an apparent deepening of the ^{12}CO absorption features where ^{13}CO lines are coincident [e.g. ^{12}CO P(5) and ^{13}CO R(7)], while the perceived continuum level is depressed in regions where ^{13}CO lines occur in between ^{12}CO lines [e.g. around^{13}CO R(4)]. To illustrate this point, the smooth red line in Fig. 2 depicts a model spectrum for the case of absorption by ^{12}CO alone, superimposed upon the echelle spectrum.

Primarily, we model the CO assuming a spherical geometry. For comparison, we consider an isothermal, plane parallel slab of absorbing CO as a secondary model. The results presented here are for the spherical model, favoured because it considers emission as well as absorption integrated over all lines of sight from Sakurai's Object, rather than a single pencil beam of light.

4.1 Spherically symmetric shell model

The CO absorption region is modelled as an expanding, spherically symmetric shell, centred on the star. Assuming dust obscuration prevents the gas from seeing the central star, we take the radiation source to be the intervening dust. The validity of this assumption is discussed in Section 5.2. By fitting a blackbody function to the 1– 5 μm continuum, we find dust temperatures of 360 ± 30 K in 2003, and 320 ± 40 K in 2004, consistent with the value of 350 ± 30 K estimated by Eyres et al. (2004). The radiative transfer model is insensitive to temperature because of the limited wavelength coverage of the echelle spectrum. We therefore fix the temperature of the dust at 320 K. The relative strengths of the low- and high-J ^{12}CO lines place constraints on the gas temperature of 320 ± 30 K. We fix this parameter in the model accordingly.

The strength of the absorption component is determined by solving the radiative transfer equation along lines of sight within the shell. We employ the CO fundamental linelist taken from Goorvitch (1994), including vibrational levels up to $v'' = 8$. All identified lines correspond to $v = 1-0$ lines, indicating no significant population of higher vibrational levels. The average measured FWHM of the CO lines is 180 km s^{-1}. We use this value to constrain velocity broadening in the model.

The model is optimized for column density N(CO) and ^{12}C/^{13}C isotopic ratio, and is fitted to the data using a minimum χ^2 test. The output value corresponding to the lowest χ^2 was established by use of the downhill simplex method of Press et al. (1992). Uncertainties in the output were estimated from the range of values produced by several iterations of the model, varying the starting points of the free parameter values. The output calculated by the model for the free parameters is given in Table 2, and compared with the results from previously published works on Sakurai's Object. An isotopic ratio of $^{12}C/^{13}C = 3.5^{+2.0}_{-1.5}$ and column density $N(\mathrm{CO}) = (7.6^{+1.5}_{-0.5}) \times 10^{16}$ cm^{-2} are determined by the fitting procedure. These output values were obtained after 48 iterations of the model. The χ^2 value that was achieved, 5.0, implies a relatively poor fit. Fixing the continuum temperature resulted in some difficulty in modelling the data, likely due to non-local thermal equilibrium population of the energy levels. A blackbody curve is a reasonable approximation to the dust continuum; slight deviation may be due to the instrumental effects.

There is a factor of 10 difference between the column density of CO in 2004, as determined by the spherical shell model, and that estimated for 2003 by Eyres et al. (2004) (Table 2). This is partially due to the weakening of the CO band between 2003 and 2004 (Fig. 1c). The 2003 estimate assumed an isothermal slab of absorbing CO, and is consistent with the value $N(\mathrm{CO}) \approx 6 \times 10^{17}$ cm^{-2} determined by our plane parallel slab model for 2004. In part, we attribute the lower column density to the fact that the spherical model integrates the absorption over all lines of sight from Sakurai's Object, hence a larger value is expected when a single line of sight is used to characterize the column density, as in the isothermal slab model. The two models find consistent ^{12}C/^{13}C isotopic ratios, independent of the geometry.

5 DISCUSSION

5.1 ^{12}C/^{13}C ratio

Possible contributors to ^{13}C observed in the ^{13}CO fundamental band lines are the ISM, the pre-existing PN and the post-VLTP ejecta from Sakurai's Object. The low ^{12}C/^{13}C ratio and high velocity of the material modelled here preclude origins in the ISM [^{12}C/^{13}C ∼ 70 (Sheffer et al. 2007)] or the evolved PN [$20 \leq {}^{12}\mathrm{C}/{}^{13}\mathrm{C} \leq 40$ (Palla et al. 2000), $v \sim 15$ km s^{-1} (Acker 1993)]. Pavlenko et al. (2004) fitted synthetic spectra to UKIRT echelle spectra of Sakurai's Object from 1998, modelling the cool stellar atmosphere in the 2.32–2.38 μm region. Using this technique, they find an isotopic ratio of $^{12}C/^{13}C = 4 \pm 1$ in material close to the star, consistent with the VLTP interpretation of Sakurai's Object. Here, we find a compatible ^{12}C/^{13}C ratio in material observed outside the dust shell in 2004.

Fig. 3 shows model spectra produced by the spherically symmetric shell model described in Section 4.1 for different ^{12}C/^{13}C ratios, superimposed upon the echelle spectrum. The best fit found by the model is depicted by the solid red line, for a ^{12}C/^{13}C ratio of 3.5. The blue dotted line corresponds to $^{12}C/^{13}C = 1$, in which the ^{13}CO lines are more pronounced than observed in Sakurai's Object [R(4)

Table 2. Values for each parameter of the spherically symmetric shell model, applied to the 2004 echelle spectra. Column two shows values calculated by the model, compared with the values from the literature in column three. Because of the variable nature of Sakurai's Object, column four gives the date of the observation to which each value from the literature corresponds. The dust temperature is determined by fitting a blackbody function to the continuum and is fixed in the model, while the temperature of the gas is determined using relative strengths of CO lines. The velocity broadening is constrained by the average FWHM of CO lines in the echelle spectra.

Parameter	Model values	Published values	Date of published observations
Dust temperature (K)	320 (fixed)	$350 \pm 30^{*}$	2003
Velocity broadening (km s^{-1})	180 (fixed)	25– 200*	2003
CO excitation temperature (K)	320 ± 30 (fixed)	$400 \pm 100^{*}$	2003
Column density ($\times 10^{16}$ cm^{-2})	$7.6^{+1.5}_{-0.5}$	70^{+30*}_{-20}	2003
^{12}C/^{13}C	$3.5^{+2.0}_{-1.5}$	1.5–5†, 4 ± 1‡, $\geq 3^{*}$, $3.2^{+3.2\S}_{-1.6}$	1996, 1998 2003, 2005

*Eyres et al. (2004), †Asplund et al. (1999), ‡Pavlenko et al. (2004), §Evans et al. (2006).

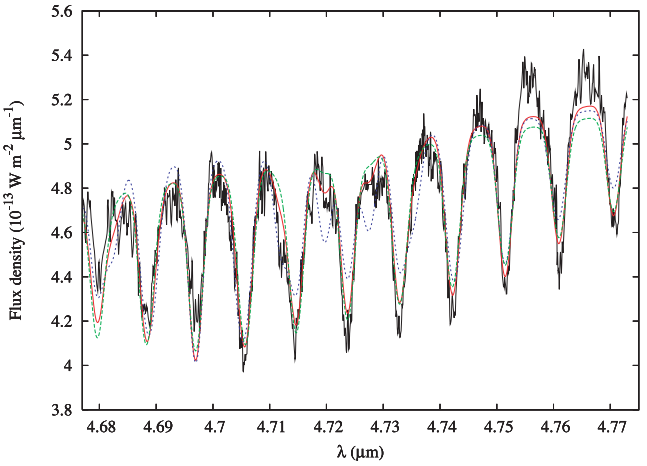

Figure 3. Spherically symmetric shell model CO spectra superimposed upon the 2004 June UKIRT echelle spectrum. Plots correspond to ^{12}C/^{13}C ratios of 10 (green dashed line), 1 (blue dotted line) and the best fit of ^{12}C/^{13}C = 3.5 (solid red line).

and R(5) in particular], whereas in the green dashed line, corresponding to ^{12}C/^{13}C = 10, the absorption features are weaker than observed and there is insufficient depression of the continuum level at wavelengths where a ^{13}CO line is expected. The isothermal slab model is in agreement with the best-fitting result of the spherically symmetric model, finding ^{12}C/^{13}C $\approx$ 3.

5.2 CO velocity

From the echelle spectrum, we measure a FWHM of the CO absorption features corresponding to a velocity broadening of 180 $\pm$ 15 km s^{-1}. A gas shell expansion velocity of 500 $\pm$ 80 km s^{-1} is obtained from the difference between the mean radial velocity of the blueward edge of the CO lines (-385 ± 80 km s^{-1}) and the systemic radial velocity ($+115$ km s^{-1}).

The absorption maximum occurs at -270 ± 15 km s^{-1}, while the mean FWZI measures 400 ± 70 km s^{-1}. Thus, assuming spherically symmetric expansion, material contributing to the redward edge of the line is moving at -70 ± 50 km s^{-1} with respect to the observer, i.e. with a velocity of 500 ± 80 km s^{-1} away from the central star, at an angle close to the plane of the sky. Similarly, the blueward edge (-470 ± 50 km s^{-1}) corresponds to gaseous motion along the line of sight to the observer. The fact that we see no emission from the limbs or the far side of the shell supports the model configuration of a star surrounded by concentric shells of dust and gas; the inferior dust shell obscures the far side of the superior gas shell, hence we detect only the blueshifted gas along the line of sight and do not see the redshifted (P Cygni) emission.

5.3 Evolution of the CO

In 1998 March, broad, blueshifted absorption of He I (1.083 μm), which was absent from a spectrum of equal resolution obtained in 1997 July, was detected around Sakurai's Object (Eyres et al. 1999). We assume the He I and CO-bearing materials were mobilized contemporaneously. Taking an expansion velocity of 500 km s^{-1} from the time of He I detection places limits on the outer gas shell radius of $9.9 \times 10^{10} \leq R_{\rm CO} \leq 1.1 \times 10^{11}$ km in 2004 June; increasing to $1.5 \times 10^{11} \leq R_{\rm CO} \leq 1.6 \times 10^{11}$ km at the time of the most recent observation in 2007. This recent gas radius is comparable with the range on the dust shell radius of 4.3×10^{10}–1.5×10^{11} km, modelled by van Hoof et al. (2007), and approximately 17 times larger than the 1997 dust radius of 8.4×10^{9} km determined by Kipper (1999). The consistent temperatures of CO and the continuum source (Table 2) indicate at least partial mixing of the gas and dust; we therefore take the radius of the CO shell to be a good approximation for that of the dust shell.

Shock acceleration to 500 km s^{-1} would result in dissociation of the CO. The absence of CO in the spectrum of Sakurai's Object in 1999 could be used to support a hypothesis of CO destruction in the 1998 onset of the fast wind, recombining by the 2000 April observation (Eyres et al. 2004). Alternatively, we suggest gentle acceleration of the gas by the dust due to radiation pressure. In this scenario, it is expected that some of the dust would precede and hence obscure the gas; the CO only becoming visible with expansion and thinning of the dust shell over time.

Assuming a thin, spherically symmetric gas shell, and taking a column density of 7.6×10^{16} cm^{-2} (derived by the spherically symmetric shell model), we place limits on the total CO ejecta mass of $4.4 \times 10^{24} \leq M_{\rm CO} \leq 5.4 \times 10^{24}$ kg (i.e. $2.2 \times 10^{-6} \leq M_{\rm CO} \leq 2.7 \times 10^{-6}$ M$_{\odot}$), dependent on the date the wind commenced. Significant asymmetry or asphericity of the nebular geometry (e.g. van Hoof et al. 2007; Kimeswenger et al. 2008) would cause this value to vary.

5.4 Dust temperature

The equilibrium temperature dust at the radius determined in Section 5.3 is ~100 K. This is based on assumptions of 1 μm graphitic

carbon grains (Tyne et al. 2002); a stellar luminosity of 3000 $L_\odot$ (Herwig 2001; Tyne et al. 2002) and an effective temperature of 5200 K (Pavlenko 2002). An equilibrium temperature of 320 K at this radius would require an impossibly high luminosity; a factor of >100 greater than predicted by the models of Herwig (2001) and Tyne et al. (2002). The CO temperature of 320 K is also inconsistent with stellar radiation. This suggests that some additional heating mechanism was operating prior to, and during, 2004. The most likely mechanism would appear to be associated with collisional heating within the wind as dust and gas velocities equalize and turbulence dissipates. The kinetic energy in the outflow is more than sufficient to heat the material to the observed temperature. The flux density at 5 μm dropped by a factor of ∼18 in the 14 months between observations in 2004 and 2005. This decline corresponds to a drop in blackbody temperature of ∼80 K, from 320 K in 2004 to ∼240 K in 2005, comparable with $\lesssim$200 K determined by Evans et al. (2006) from *Spitzer* observations at 20 μm in 2005 April. This is a much larger drop than in the years just prior to and subsequent to 2004 and 2005 (Fig. 1a) and may indicate the rapid weakening of this additional heating process.

6 CONCLUSIONS

Observations in the 1–5 μm region show weakening of the CO and continued cooling of the dust surrounding Sakurai's Object between 2003 and 2007, with a particularly marked temperature decrease between 2004 and 2005. The 2004 dust temperature is ∼200 K hotter than can be accounted for by stellar radiation alone.

From an echelle spectrum of CO absorption features around 4.7 μm, we determine a wind velocity of $500 \pm 80\,\mathrm{km\,s^{-1}}$, which we use to estimate an outer gas shell radius of $9.9 \times 10^{10} \leq R_{\mathrm{CO}} \leq 1.1 \times 10^{11}$ km ($1.4 \times 10^5 \leq R_{\mathrm{CO}} \leq 1.6 \times 10^5\,R_\odot$) in 2004. With consistent gas and dust temperatures (320 ± 30 and 320 ± 40 K, respectively), we believe the two components to be at least partially mixed. Assuming continuous, uninterrupted expansion of the CO away from the central star at constant velocity, the gas shell radius would have reached $1.5 \times 10^{11} \leq R_{\mathrm{CO}} \leq 1.6 \times 10^{11}$ km ($2.2 \times 10^5 \leq R_{\mathrm{CO}} \leq 2.3 \times 10^5\,R_\odot$) by the time of the most recent observation of Sakurai's Object in 2007 June. We measure a velocity of peak absorption of $-270 \pm 15\,\mathrm{km\,s^{-1}}$, comparable with $-290 \pm 30\,\mathrm{km\,s^{-1}}$ obtained by Eyres et al. (2004) in 2003.

By modelling the CO fundamental in a spherically symmetric shell of material surrounding Sakurai's Object, we have determined an isotopic ratio of $^{12}\mathrm{C}/^{13}\mathrm{C} = 3.5^{+2.0}_{-1.5}$. Application of a simple isothermal slab model of absorbing CO also yields $^{12}\mathrm{C}/^{13}\mathrm{C} \approx 3$. These results are consistent with earlier estimates of this isotopic ratio in this system (Asplund et al. 1999; Eyres et al. 2004; Pavlenko et al. 2004; Evans et al. 2006). In particular, agreement with the atmospheric simulations of Pavlenko et al. (2004) demonstrates this low ratio as being consistent with material having been ejected from the central star during the VLTP event and being swept out with the fast wind, rather than forming part of the old PN, or existing in the intervening ISM.

ACKNOWLEDGMENTS

HLW acknowledges studentship support from the University of Central Lancashire. MTR acknowledges support from the University of Central Lancashire. TRG is supported by the Gemini Observatory, which is operated by the Association of Universities for Research in Astronomy, Inc., on behalf of the international Gemini partnership of Argentina, Australia, Brazil, Canada, Chile, the United Kingdom and the United States of America. Some of the data reported here were obtained as part of the UKIRT Service Programme. The United Kingdom Infrared Telescope is operated by the Joint Astronomy Centre on behalf of the Science and Technology Facilities Council of the UK.

REFERENCES

Acker A., 1993, Acta Astron., 43, 419
Asplund M., Lambert D. L., Kipper T., Pollacco D., Shetrone M. D., 1999, A&A, 343, 507
Duerbeck H. W., Benetti S., 1996, ApJ, 468, L111
Duerbeck H. W., Benetti S., Gautschy A., van Genderen A. M., Kemper C., Liller W., Thomas T., 1997, AJ, 114, 1657
Evans A. et al., 2006, MNRAS, 373, L75
Eyres S. P. S., Smalley B., Geballe T. R., Evans A., Asplund M., Tyne V. H., 1999, MNRAS, 307, L11
Eyres S. P. S., Geballe T. R., Tyne V. H., Evans A., Smalley B., Worters H. L., 2004, MNRAS, 350, L9
Goorvitch D., 1994, ApJ, 95, 535
Hajduk M. et al., 2005, Sci, 308, 231
Herwig F., 2001, ApJ, 554, L71
Iben I., Tutukov A. V., Yungelson L. R., 1996, ApJ, 456, 750
Kimeswenger S., Koller J., 2002, Ap&SS, 279, 149
Kimeswenger S., Zijlstra A. A., van Hoof P. A. M., Hajduk M., Lechner M. F. M., van de Steene G. C., Gesicki K., 2008, in Corradi R. L. M., Manchado A., Soker N., eds, Proc. Asymmetric Planetary Nebulae IV, in press (arXiv:0804.4058)
Kipper T., 1999, Balt. Astron., 8, 483
Nakano S., Sakurai Y., Hazen M., McNaught R. H., Benetti S., Duerbeck H. W., Cappellaro E., Leibundgut B., 1996, IAU Circ. 6322
Palla F., Bachiller R., Stanghellini L., Tosi M., Galli D., 2000, A&A, 355, 69
Pavlenko Y. V., 2002, Ap&SS, 279, 91
Pavlenko Y. V., Geballe T. R., Evans A., Smalley B., Eyres S. P. S., Tyne V. H., Yakovina L. A., 2004, A&A, 417, L39
Press W. H., Flannery B. P., Teukolsky S. A., Vetterling W. T., 1992, Numerical Recipes in FORTRAN. Cambridge Univ. Press, Cambridge
Sheffer Y., Rogers M., Federman S. R., Lambert D. L., Gredel R., 2007, ApJ, 667, 1002
Tokunaga A. T., 2000, in Cox A. N., ed., Allen's Astrophysical Quantities. New York, Springer, p. 143
Tyne V. H., Eyres S. P. S., Geballe T. R., Evans A., Smalley B., Duerbeck H. W., Asplund M., 2000, MNRAS, 315, 595
Tyne V. H., Evans A., Geballe T. R., Eyres S. P. S., Smalley B., Duerbeck H. W., 2002, MNRAS, 334, 875
van Hoof P. A. M., Hajduk M., Zijlstra A. A., Herwig F., Evans A., Van de Steene G. C., Kimeswenger S., 2007, A&A, 471, L7

This paper has been typeset from a TEX/LATEX file prepared by the author.